THE JOURNAL OF BIOLOGICAL CHEMISTRY VOL. 282, NO. 23, pp. 16924–16933, June 8, 2007

Insights into How CUB Domains Can Exert Specific Functions while Sharing a Common Fold

CONSERVED AND SPECIFIC FEATURES OF THE CUB1 DOMAIN CONTRIBUTE TO THE MOLECULAR BASIS OF PROCOLLAGEN C-PROTEINASE ENHANCER-1 ACTIVITY[*][S]

Received for publication, February 23, 2007, and in revised form, April 12, 2007 Published, JBC Papers in Press, April 19, 2007, DOI 10.1074/jbc.M701610200

Guillaume Blanc, Bernard Font, Denise Eichenberger, Christophe Moreau[1], Sylvie Ricard-Blum, David J. S. Hulmes[2], and Catherine Moali

From the Institut de Biologie et Chimie des Protéines, CNRS/Université Claude Bernard Lyon 1, Unité Mixte de Recherche 5086, Institut Fédératif de Recherche 128 Biosciences Lyon Gerland, 7 Passage du Vercors, 69367 Lyon cedex 7, France

Procollagen C-proteinase enhancers (PCPE-1 and -2) are extracellular glycoproteins that can stimulate the C-terminal processing of fibrillar procollagens by tolloid proteinases such as bone morphogenetic protein-1. They consist of two CUB domains (CUB1 and -2) that alone account for PCPE-enhancing activity and one C-terminal NTR domain. CUB domains are found in several extracellular and plasma membrane-associated proteins, many of which are proteases. We have modeled the structure of the CUB1 domain of PCPE-1 based on known three-dimensional structures of CUB-containing proteins. Sequence alignment shows conserved amino acids, notably two acidic residues (Asp-68 and Asp-109) involved in a putative surface-located calcium binding site, as well as a conserved tyrosine residue (Tyr-67). In addition, three residues (Glu-26, Thr-89, and Phe-90) are found only in PCPE CUB1 domains, in putative surface-exposed loops. Among the conserved residues, it was found that mutations of Asp-68 and Asp-109 to alanine almost completely abolished PCPE-1 stimulating activity, whereas mutation of Tyr-67 led to a smaller reduction of activity. Among residues specific to PCPEs, mutation of Glu-26 and Thr-89 had little effect, whereas mutation of Phe-90 dramatically decreased the activity. Changes in activity were paralleled by changes in binding of different PCPE-1 mutants to a mini-procollagen III substrate, as shown by surface plasmon resonance. We conclude that PCPE-stimulating activity requires a calcium binding motif in the CUB1 domain that is highly conserved among CUB-containing proteins but also that PCPEs contain specific sites that could become targets for the development of novel anti-fibrotic therapies.

CUB[3] domains are widely occurring structural motifs, found almost exclusively in extracellular and plasma membrane-associated proteins. These proteins are involved in a wide range of biological functions, including complement activation (1, 2), developmental patterning (3, 4), tissue repair (5), axon guidance and angiogenesis (6, 7), cell signaling (8), fertilization (9), hemostasis (10), inflammation (11), neurotransmission (12), receptor-mediated endocytosis (13, 14), and tumor suppression (15, 16). Many CUB domain-containing proteins are proteases (1, 2, 5, 10, 17–19). Although the roles of the CUB domains are largely unexplored, a number of them have been shown to be involved in oligomerization and/or recognition of substrates and binding partners.

The protein families from which the CUB domain derives its name are the complement serine proteases C1r, C1s, MASP-1, MASP-2, and MASP-3 and the bone morphogenetic protein-1/tolloid metalloproteases BMP-1, mTLD, mTLL-1, and mTLL-2 (or their counterparts xolloids, tolloids, and SpAN/BP10 in *Xenopus*, *Drosophila*, and sea urchin, respectively). Each consists of a catalytic domain (either N-terminal in tolloids or C-terminal in complement proteases) together with several CUB domains interspersed by calcium-binding EGF domains. In the case of the complement proteases, the CUB domains mediate dimerization and binding to the collagen-like regions of C1q (for C1r/C1s) and MBL or L- and H-ficolin (for MASP-2). The three-dimensional structures of the CUB1-EGF fragment of C1s, its homologue in MASP-2 (which also occurs as the alternatively spliced product MAp19) as well as the CUB1-EGF-CUB2 fragment of MASP-2 have been determined (20–22). These studies have revealed the presence of a calcium binding site in the CUB1 domains of both C1s and MAp19, within the loops distal to the EGF domain. In the case of MAp19, site-directed mutagenesis has shown the involvement of this region in binding to MBL and L-ficolin (21).

The BMP-1/tolloid-related metalloproteinases (BMP-1, mTLD, mTLL-1, and mTLL-2 in mammals) are members of the astacin family (M12A) of the metzincin subclan MA(M) (23, 24). Following the pro-region, which is removed by a furin-like

* This work was supported by the Région Rhône-Alpes, the European Commission (Contract No. NMP2-CT-2003-504017), the Ligue Contre le Cancer, Engelhard (Lyon), the Centre National de la Recherche Scientifique and the Université Claude Bernard Lyon 1. The costs of publication of this article were defrayed in part by the payment of page charges. This article must therefore be hereby marked "*advertisement*" in accordance with 18 U.S.C. Section 1734 solely to indicate this fact.

[S] The on-line version of this article (available at http://www.jbc.org) contains supplemental Table S1 and Figs. S1 and S2.

[1] Present address: Commissariat à l'Energie Atomique-Grenoble/Département Réponse et Dynamique Cellulaires/Laboratoire de Biophysique Moléculaire et Cellulaire, CNRS Unité Mixte de Recherche 5090, 38054 Grenoble, France.

[2] To whom correspondence should be addressed. Tel.: 33-472-722-667; Fax: 33-472-722-604; E-mail: d.hulmes@ibcp.fr.

[3] The abbreviations used are: CUB, module found in complement subcomponents C1r/C1s, Uegf, and BMP-1; BMP-1, bone morphogenetic protein-1; mTld, mammalian tolloid; mTLL-1, mammalian tolloid-like 1; mTLL-2, mammalian tolloid-like 2; PCP, procollagen C-proteinase; PCPE, PCP enhancer.

proteinase, each variant consists of an astacin domain followed by a C-terminal region consisting of variable numbers of CUB and calcium-binding EGF domains. In the case of BMP-1, this C-terminal region has the domain organization CUB1-CUB2-EGF1-CUB3, whereas in the longer mTLD splice variant it is CUB1-CUB2-EGF1-CUB3-EGF2-CUB4-CUB5. Variants mTLL-1 and mTLL-2 share the same domain structure as mTLD but are products of separate genes. These proteinases cleave a large number of substrates, including the fibrillar procollagens I, II, III, V, and XI, the non-fibrillar procollagen VII, prolysyl oxidases, the laminin 5 γ2 chain, dentin matrix protein-1, precursor forms of the small leucine rich proteoglycans biglycan and osteoglycin, the heparan sulfate proteoglycan perlecan, growth factors myostatin and GDF11, the growth factor antagonist chordin (24), and latent transforming growth factor-β-binding protein (LTBP), which controls transforming growth factor-β activity (25).

There is increasing evidence that tolloid proteinase activity is subject to regulation by a variety of extracellular proteins. During developmental patterning, for example, it has recently been shown that the frizzled-related protein sizzled is an endogenous inhibitor of BMP-1 (3, 26), whereas complex formation involving the protein-twisted gastrulation stimulates the activity of BMP-1 on chordin and exposes a new cleavage site (27). Procollagen C-proteinase enhancers (PCPE-1 and -2) also stimulate the activities of tolloid proteinases, in a substrate-specific manner (28). PCPE-1 has no effect on cleavage of several BMP-1 substrates (28), including chordin (29), prolysyl oxidase, osteoglycin, the laminin 5 γ2 chain, procollagen VII, and the N-propeptide region of procollagen V. In contrast, both PCPE-1 and -2 have been shown to stimulate the activities of tolloid proteinases during cleavage of the C-propeptide regions of the major fibrillar procollagens (types I, II, and III) (28, 30, 31). Targeted deletion of the PCPE-1 gene has recently been shown to lead to aberrant collagen fibril formation and impaired biomechanical properties of bone tissue (32).

PCPEs are extracellular glycoproteins, devoid of intrinsic proteolytic activity, consisting of two CUB domains followed by a C-terminal NTR domain (31). Enzymatic removal of the NTR domain has no effect on enhancement of tolloid proteinase activity, showing that this is a property of the CUB domain region (33, 34). Although the mechanism of action of PCPEs is not well understood, this probably involves binding to the substrate, because maximum enhancing activity is found for PCPE: procollagen molar ratio of at least 1:1. BIAcore studies have shown that PCPE-1 binds to both the C-propeptide region as well as elsewhere in the procollagen molecule (35). Recent studies using a miniprocollagen III substrate have shown that enhancing activity is unaffected by removal of essentially all of the triple-helical region using highly purified bacterial collagenase (28). Taken together, these data suggest that PCPE-1 binds to the non-triple-helical telopeptide region N-terminal to the BMP-1 cleavage site, in addition to the C-propeptide region, thereby inducing a conformational change that facilitates the action of BMP-1. It is also possible that PCPE-1 binds to tolloid proteinases, as recently shown for mTLL-1 (36). To further explore the mechanism of action of PCPE-1, it is important to identify recognition sites within the CUB domains involved in enhancing activity. Here, we show that these involve a putative calcium binding site in the CUB1 domain, as well as a site specific to the CUB1 domain of PCPEs.

TABLE 1

Sequences of forward primers used to generate the PCPE-1 mutants

Reverse primers had the complementary sequences. Mutated codons are underlined.

E26A	5′-GTG GCA AGT GCG GGG TTC CCC-3′
Y67A	5′-GCC TGC CGC GCC GAT GCT CTG-3′
D68A	5′-GCC TGC CGC TAC GCT GCT CTG GAG G-3′
T89A	5′-TTT TGT GGG GCC TTC CGG CCT G-3′
F90A	5′-TGT GGG ACC GCC CGG CCT GCG-3′
D109A	5′-AGG ATG ACG ACG GCT GAG GGC ACA GGA G-3′

EXPERIMENTAL PROCEDURES

Molecular Modeling—The three-dimensional model of the CUB1 domain of human PCPE-1 (residues 12–124, numbered from the N terminus of the mature protein, *i.e.* after cleavage of the signal peptide) was built with the comparative molecular modeling program Geno3D (37), using the CUB domain structure with the highest sequence homology, namely the CUB2 domain of rat MASP-2 (22). Ten three-dimensional structures were generated and superimposed with the ANTHEPROT three-dimensional package (38). The quality of the models was assessed using PROCHECK, and the most representative model, with the lowest energy, was selected.

Recombinant Proteins—The BMP-1 FLAG construct was obtained by PCR using the BMP-1 cDNA inserted in pCEP4 as a template (28). The FLAG sequence was inserted immediately contiguous to the BMP-1 sequence before the STOP codon. After sequencing and transfection in 293-EBNA cells, a clone was selected that gave the highest BMP-1 level of expression. This clone was used for further amplification and production of the protein.

For site-directed mutagenesis and production of PCPE mutants, an 8-histidine tag was inserted by PCR into the human PCPE-1 cDNA (28), before the STOP codon, and the PCR product was cloned into pCR-Blunt II TOPO (Invitrogen). This construct was used as a template to generate all the PCPE-1 mutants using the QuikChange™ site-directed mutagenesis kit from Stratagene, according to the manufacturer's protocol. Overlapping oligonucleotides (Table 1) were purchased from MWG-BIOTECH (Courtaboeuf, France). The mutated inserts were then subcloned into pCEP4 (Invitrogen) using the KpnI and BamHI sites for semi-stable transfections into 293-EBNA cells (28). The sequences of all mutants were confirmed by double-stranded DNA sequencing (Genome Express, France).

Protein Purification—For BMP-1-FLAG, the first purification step (Reactive Green) was as previously described for BMP-1 (28). BMP-1-FLAG-containing fractions (according to SDS-PAGE) were dialyzed against Buffer A (20 mM Hepes, pH 7.4, 2.5 mM $CaCl_2$, 0.02% octyl-β-D-glucopyranoside) plus 0.25 M NaCl, and loaded onto an Anti-FLAG M2-agarose affinity column (Sigma) equilibrated with the same buffer. After washing with Buffer A plus 0.5 M NaCl, bound BMP-1-FLAG was eluted using 0.25 mg/ml FLAG peptide dissolved in Buffer A plus 0.5 M NaCl, then extensively dialyzed against the same buffer without peptide. We checked that the purified protein was devoid of endogenous PCPEs.

For His-tagged PCPE-1 and its mutants, conditioned medium was centrifuged to remove cell debris and incubated with nickel-agarose equilibrated with 50 mM sodium phosphate, pH 8.0, 0.3 M NaCl (buffer B). The resin was then packed into a column and washed with buffer B containing 10 mM imidazole. The protein was eluted with 0.25 M imidazole in buffer B, and extensively dialyzed against phosphate-buffered saline.

Enzymatic Activities—BMP-1 activity was measured as previously described (28), using either [^{3}H]procollagen I isolated from chick embryo fibroblasts or mini-procollagen III produced in 293 EBNA cells, as specified in the figure legends.

Circular Dichroism—Far-UV (190–250 nm) CD measurements were carried out using thermostatted 0.2-mm path length quartz cells in a Jobin-Yvon CD6 instrument, calibrated with aqueous *d*-10-camphorsulfonic acid. Proteins (0.3–1 mg/ml) were analyzed at 25 °C in 20 mM KH_2PO_4/NaOH, 150 mM NaF, pH 7.2. Spectra were measured with a wavelength increment of 0.2 nm, integration time of 1 s, and bandpass of 2 nm. Protein concentrations were determined by absorbance at 280 nm (using absorbances calculated for each mutant based on the amino acid sequence) as well as by the Bradford assay, normalizing the latter to a known concentration of wild-type PCPE-1. Secondary structure analysis was carried out on the DICHROWEB server (39) using the CDSSTR program.

Fluorescence—Intrinsic fluorescence was measured at 25 °C using a Photon Technology International instrument with a 10-mm path length quartz cell. Emission was recorded between 295 and 400 nm after excitation at 280 nm (excitation slits: 8 nm; emission slits: 4 nm) with a scanning rate of 1 nm/s. PCPE-1 was dialyzed against 20 mM HEPES, pH 7.4, 0.15 M NaCl and diluted to 2.5 μM in a total volume of 500 μl of the same buffer. EGTA and $CaCl_2$ were added in 1-μl volumes. Fluorescence spectra were recorded 5 min after each addition and corrected for fluorescence of the buffer (containing or not EGTA and/or calcium). The effect of EGTA and calcium was also measured on a control solution of 5.4 μM *N*-acetyltryptophan amide (NATA) to check that changes in fluorescence were not due to absorption by added compounds (40).

Surface Plasmon Resonance—Surface plasmon resonance analyses were carried out on a BIAcore 3000 instrument. Mini-procollagen III was covalently coupled to a CM4 sensor chip after activation with *N*-hydroxysulfosuccinimide and 1-ethyl-3-[3-dimethylaminopropyl] carbodiimide hydrochloride (amine coupling) and injection in 10 mM sodium acetate, pH 5. Unreacted groups on the surface were neutralized with ethanolamine hydrochloride. The whole procedure was performed at a flow rate of 5 μl/min. A control flow cell was prepared similarly except that the mini-procollagen III solution was replaced by 10 mM sodium acetate, pH 5. The signal recorded on the control flow cell was automatically subtracted from those of the other flow cells. Prior to analysis, ligands were dialyzed against HBS-P (10 mM HEPES, pH 7.4, 0.15 M NaCl, and 0.005% P20 surfactant), and binding was monitored at 25 °C in the same buffer (containing or not 5 mM $CaCl_2$) at a flow rate of 60 μl/min. Regeneration was carried out with 2 M guanidinium chloride when experiments were run in the absence of added calcium or with sequential injections of 0.25 M EDTA and 2 M guanidinium chloride in the presence of 5 mM calcium. Kinetic data were analyzed using BIAevaluation 4.1 software.

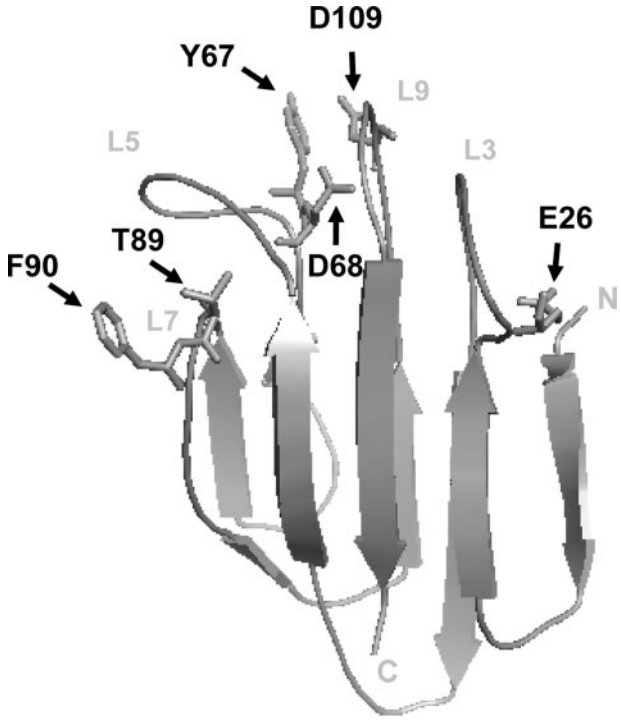

FIGURE 1. **Structural model of the CUB1 domain of human PCPE-1.** The model was generated using the known structure of the rat MASP-2 CUB2 domain as a template. Residues either highly conserved in CUB domains (Tyr-67, Asp-68, and Asp-109) or specific to the CUB1 domains of PCPEs (Glu-26, Thr-89, and Phe-90) are indicated. Also shown are loops L3, L5, L7, and L9 previously described in the CUB1 domain structures of human C1s and MAp19, as well as the N and C termini. The figure was prepared using PyMOL.

RESULTS

Identification of Target Residues—As sequence alignment with CUB domains of known three-dimensional structure (20–22, 41) showed the strongest homology (33% sequence identity) with the CUB2 domain of rat MASP-2 (22), this structure was used for molecular modeling of the human PCPE-1 CUB1 domain. As shown in Fig. 1, the predicted structure is a β-sandwich, where the root mean square deviation is 1.12 Å with respect to the template. Fig. 2 shows a sequence alignment of selected CUB domains in PCPEs and related human proteins, compared with the positions of sheets and loops in known structures, as illustrated by the MAp19 CUB domain (21). Four large loops are present on the upper face of the structure (*loops L3*, *L5*, *L7*, and *L9*, Fig. 1), as being exposed to solvent and accessible for ligand binding.

Because previous studies on MAp19 indicated the importance of the loop regions in CUB domain interactions with MBL and L-ficolin (21), we sought to identify residues involved in the interaction of the PCPE-1 CUB1 domain with procollagens by analysis of conserved and specific residues in the loops in the model shown in Fig. 1. As shown in Fig. 2, and as previously pointed out by Gregory *et al.* (20), CUB domains from several proteins, including the CUB1 domain of PCPE-1, contain three highly conserved acidic residues (Glu-45, Asp-53, and Asp-98 in C1s; Glu-52, Asp-60, and Asp-105 in MAp19; and Glu-60, Asp-68, and Asp-109 in PCPE-1) that have been shown to be

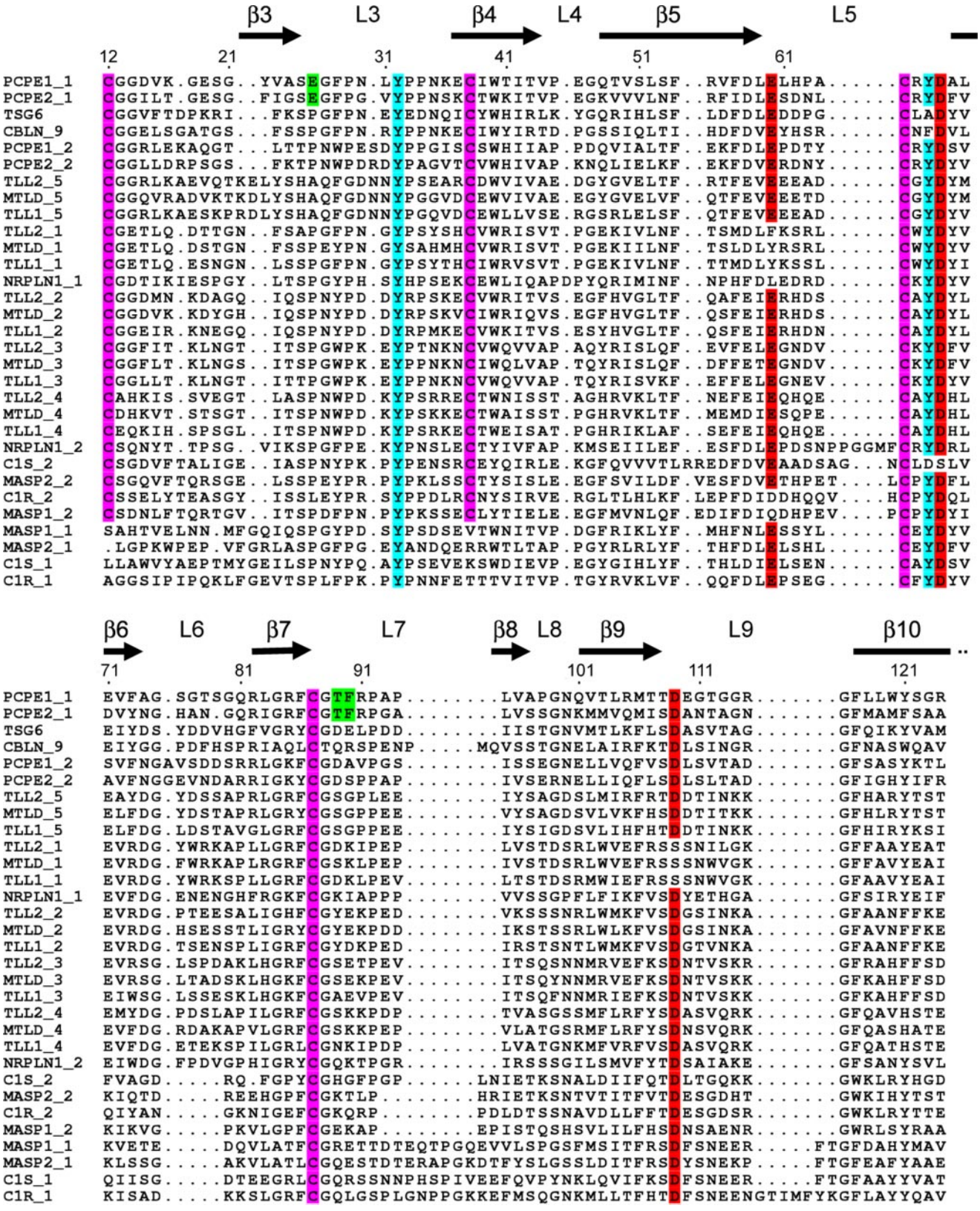

FIGURE 2. **Alignment of CUB domains.** Amino acid sequences of selected extracellular human proteins were aligned using ClustalW. Conserved cysteines are highlighted in *pink*, tyrosines in *blue*, and acidic residues involved in calcium coordination (based on known three-dimensional structures) in *red*. Residues in surface loops specific to PCPE CUB1 domains are highlighted in *green*. Secondary structure elements (*β* sheets and loops) are also shown based on the structure of the MAp19 CUB domain (equivalent to MASP2-CUB1). Residue numbering refers to the CUB1 domain of mature PCPE-1 (*i.e.* after cleavage of the signal peptide). Individual CUB domains in multi-CUB domain proteins are distinguished by numbers starting at the N terminus. *TSG6*, tumor necrosis factor-stimulated gene *6*; *CBLN*, cubulin; *NRPLN1*, neuropilin-1. The figure was prepared using ESPript (53).

involved in the coordination of a calcium atom in the three-dimensional structures of C1s (20) and MAp19 (21). This calcium binding site is formed by the loops located on the upper face of the β-sandwich structure (Fig. 1). Furthermore, a tyrosine residue involved in stabilizing this calcium binding site through formation of an H-bonding network (Tyr-17 in C1s, Tyr-24 in MAp19) is also conserved in PCPE-1 (Tyr-32). These sequence identities therefore point to a putative calcium binding site in PCPE-1. In addition to Glu-60, Asp-68, and Asp-109, Tyr-67 in PCPE-1 CUB1 (Tyr-52 in C1s and Tyr-59 in MAp19) is also conserved and is predicted to occur in the vicinity of this putative calcium binding site, with its side chain exposed to solvent (Fig. 1).

Calcium coordination involves one side-chain oxygen of Glu-45 in C1s or its homologue Glu-52 in MAp19. In contrast, while Asp-53 and Asp-98 in C1s, and Asp-60 and Asp-105 in MAp19, both contribute to calcium coordination, there are differences in the actual atoms involved, involving both side-chain and carbonyl oxygens (20, 21). For these reasons Glu-60 and Tyr-32 in PCPE-1 CUB1 are likely to be intimately involved in calcium binding, whereas Tyr-67, Asp-68, and Asp-109, although strongly conserved in CUB domains and also likely to be involved in calcium binding, might also be available for interactions with procollagens.

To identify residues specific to PCPE CUB1 domains that might be involved in binding to procollagens, we carried out a sequence alignment with CUB domains most closely related, in the data base of human proteins, to those of PCPEs. As shown in Fig. 2, only three surface-exposed residues specific to the CUB1 domains of PCPE-1 and -2 were found within loops L3, L5, L7, and L9: Glu-26, Thr-89, and Phe-90. We therefore identified six residues potentially involved in interactions with procollagens, including three conserved residues (Tyr-67, Asp-68, and Asp-109) and three specific to PCPE CUB1 domains (Glu-26, Thr-89, and Phe-90).

Production and Characterization of Site-directed Mutants—To determine the roles of the residues identified by the molecular modeling, we produced a series of recombinant site-directed mutants and tested their effects on PCPE-1 enhancement of procollagen processing by BMP-1. Alanine mutations were systematically introduced into recombinant full-length human PCPE-1 followed by expression in 293-EBNA cells. All constructs contained a polyhistidine tag at the C terminus of the NTR domain, both for ease of purification and also to separate the recombinant protein from traces of endogenous wild-type PCPE-1 produced by these cells (28). The presence of the His tag had no effect on the tolloid proteinase-enhancing activity of PCPE-1 (data not shown). As shown in supplemental Fig. S1, all mutants were expressed and efficiently purified by nickel-agarose chromatography. In addition, CD analysis showed no major changes in secondary structure as a result of the mutations (supplemental Fig. S2 and Table S1).

Residues Involved in PCPE-enhancing Activity—Enhancing activity was initially tested using the previously described mini-procollagen III substrate (28), which consists of the C-propeptide region, the C-telopeptide region, and the 33 most C-terminal (Gly-Xaa-Yaa) triplets of human procollagen III, in the presence of recombinant, human BMP-1. As shown in Fig. 3,

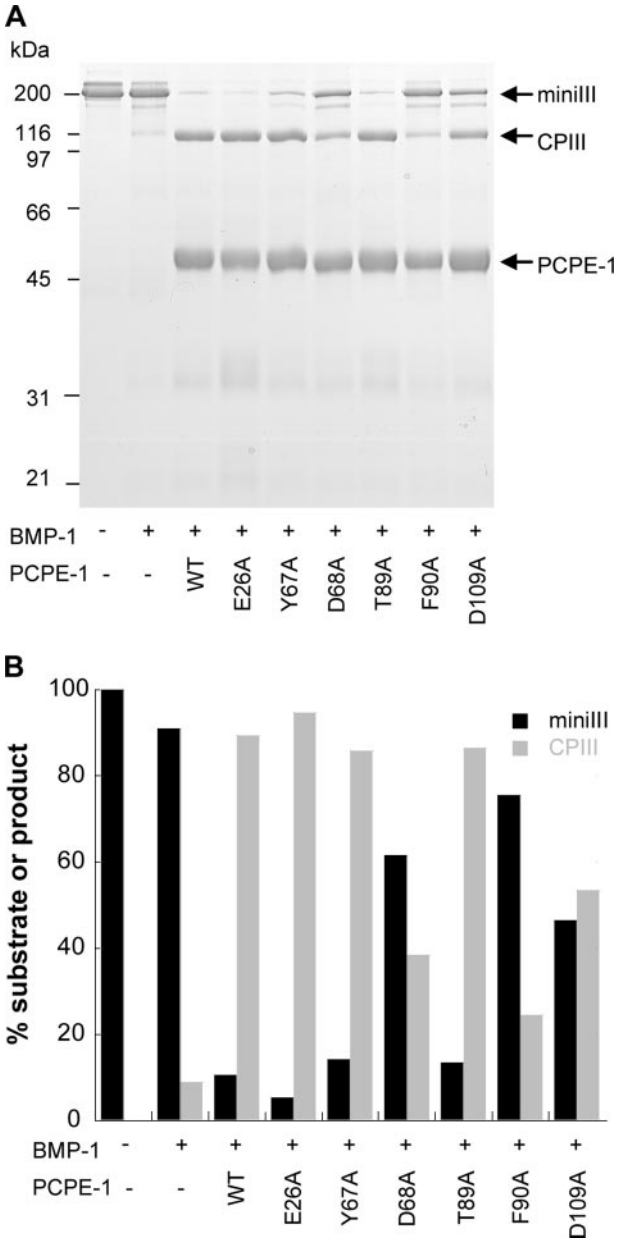

FIGURE 3. **Effects of PCPE-1 mutations on BMP-1-enhancing activity using a mini-procollagen III substrate.** *A*, mini-procollagen III (19 pmol) was incubated for 2 h at 37 °C in the presence or absence of 19 pmol of wild-type His-tagged PCPE-1 or its mutants, in 50 μl of assay buffer, with or without 0.4 pmol of BMP-1, followed by analysis in 10% acrylamide gels under nonreducing conditions and staining with Coomassie Blue. *B*, densitometric analysis of the gel shown in *A*. Results are expressed as percentages of the total substrate (mini-procollagen III) plus product (C-propeptide III). *MiniIII*, mini-procollagen III; *CPIII*, C-propeptide III.

the presence of PCPE-1, at an equimolar ratio with regard to the substrate, enhanced the activity of BMP-1 on mini-procollagen III, as previously reported (28). As judged both qualitatively and quantitatively from the Coomassie Blue-stained gels (Fig. 3), the degree of enhancement appeared similar to wild type for the PCPE CUB1-specific E26A and T89A mutants. In contrast, the PCPE CUB1-specific F90A mutation led to an almost total loss of PCPE-enhancing activity. Mutation of the conserved residues Asp-68 and Asp-109, likely to be involved with the putative calcium binding site, led to a marked drop in enhancing

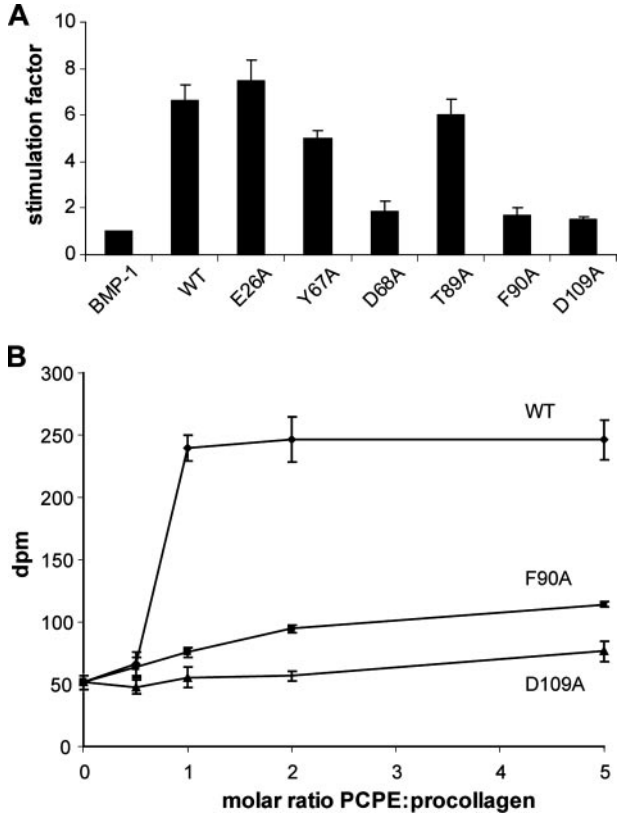

FIGURE 4. **Effects of PCPE-1 mutations on BMP-1-enhancing activity using a radioactive procollagen I substrate.** *A*, [^{3}H]tryptophan-labeled procollagen I (12.5 pmol) was incubated in 100 μl of assay buffer for 1 h and 30 min at 37 °C, with or without 12.5 pmol of wild-type PCPE-1 or its mutants, in the presence of 0.24 pmol of BMP-1-FLAG, followed by scintillation counting of released C-propeptides. The stimulation factor is the ratio of BMP-1 activity in the absence and presence of PCPE-1. Means ± S.D.s are indicated, for three independent measurements. *B*, BMP-1 activity (dpm) as a function of the molar ratio PCPE-1:[^{3}H]procollagen I for wild-type PCPE-1 and for the F90A and D109A mutants, with fixed amounts of enzyme and substrate. The conditions were the same as in *A* except that the amounts of PCPE-1 and mutants were varied. Means ± S.D.s are indicated, for three independent measurements.

activity. The Y67A mutation was associated with a relatively small drop in enhancing activity.

To obtain additional quantitative data on the effects of the mutations, PCPE-1-enhancing activity was measured using a [^{3}H]tryptophan-labeled procollagen I substrate, as described (27, 42), except that BMP-1 FLAG was used instead of BMP-1. The presence of the C-terminal FLAG had no effect on BMP-1 activity (43). The extent of enhancement, measured as the ratio of BMP-1 activity in the presence and absence of PCPE-1, is shown in Fig. 4*A*. The results confirm those obtained with the mini-procollagen III substrate. The E26A and T89A mutations had little effect on enhancing activity, although E26A appeared to be slightly more active (+14%) and T89A slightly less active (−11%) than the control. In contrast, the Y67A mutation led to a pronounced decrease (−29%), whereas mutations D68A, F90A, and D109A almost completely abolished enhancing activity (−85%, −88%, and −90%, respectively).

To determine whether the loss in enhancing activity was due to a change in the optimum enhancer:substrate stoichiometry, the enhancing activities of two of the most affected mutants (F90A and D109A) were measured as a function of the ratio of enhancer to [^{3}H]procollagen I, in comparison with wild-type PCPE-1. As expected (30, 44), maximum enhancement with wild-type PCPE-1 was obtained at an enhancer:substrate ratio of 1:1. In contrast, for the mutants F90A and D109A, increasing the enhancer:substrate ratio up to 5:1 led only to a gradual increase in enhancing activity, with no sign of a plateau, and enhancing activity remained considerably less than that of the control (Fig. 4*B*).

Effects of Mutations on PCPE-1 Binding to Procollagen—To determine whether the observed changes in PCPE-1-enhancing activity of the mutants were associated with changes in binding affinity for the substrate, the interactions of wild-type and mutant forms of PCPE-1 with immobilized mini-procollagen III were measured using surface plasmon resonance technology (BIAcore). As expected, injection of wild-type PCPE-1 over immobilized mini-procollagen III resulted in concentration-dependent specific binding to the surface (data not shown). As shown in Fig. 5, the binding of PCPE-1 to the immobilized mini-procollagen III was initially fast and then slowed down without reaching a plateau, even when the injection time was doubled. This sensorgram is reminiscent of the sensorgrams previously obtained when the C-propeptides of procollagen I or III were injected over immobilized PCPE-1 (35). The various PCPE-1 mutants were then sequentially injected over the same regenerated mini-procollagen III surface at a fixed concentration of 100 nM, in the absence or presence of 5 mM Ca^{2+} (Fig. 5). At first glance, the most striking effect of calcium was the shape of the sensorgrams: association was even faster with calcium, whereas dissociation was much slower especially for wild-type PCPE-1 and E26A. Moreover, absolute responses were significantly higher for all the proteins, even for the mutants that gave a very low signal in the absence of calcium (D68A and F90A). Altogether, these results suggest that the interaction between PCPE-1 and mini-procollagen III is much tighter in the presence of calcium, and this remains true for mutants of the putative calcium binding site (D68A and D109A).

With regard to mutations having little effect on PCPE-enhancing activity, binding of E26A to mini-procollagen III was similar to control in both conditions but binding of T89A in the absence of calcium seemed significantly impaired. The binding was partially restored in the presence of calcium to reach a level (−11% at the end of injection compared with wild type), which correlates well with the small drop in enhancing activity observed with this mutant. Concerning the mutations having major effects on enhancing activity, as shown in Fig. 5, the extent of binding of the Y67A mutant was less than wild-type, in agreement with the drop in enhancing activity (Figs. 3 and 4), whereas binding of mutants D68A, F90A, and D109A to mini-procollagen III was even lower (although partially rescued by calcium addition), consistent with the virtual abolition of enhancing activity (Figs. 3 and 4). Thus, in general, changes in binding affinity to mini-procollagen III mirrored the changes in enhancing activity introduced by the mutations.

Surface plasmon resonance was also used to determine dissociation constants for PCPE-1 and its mutants. On the same sensor chip (with a low level of immobilization to avoid mass transfer limitations), the concentrations of injected PCPE-1 and mutants were varied to obtain kinetic and affinity con-

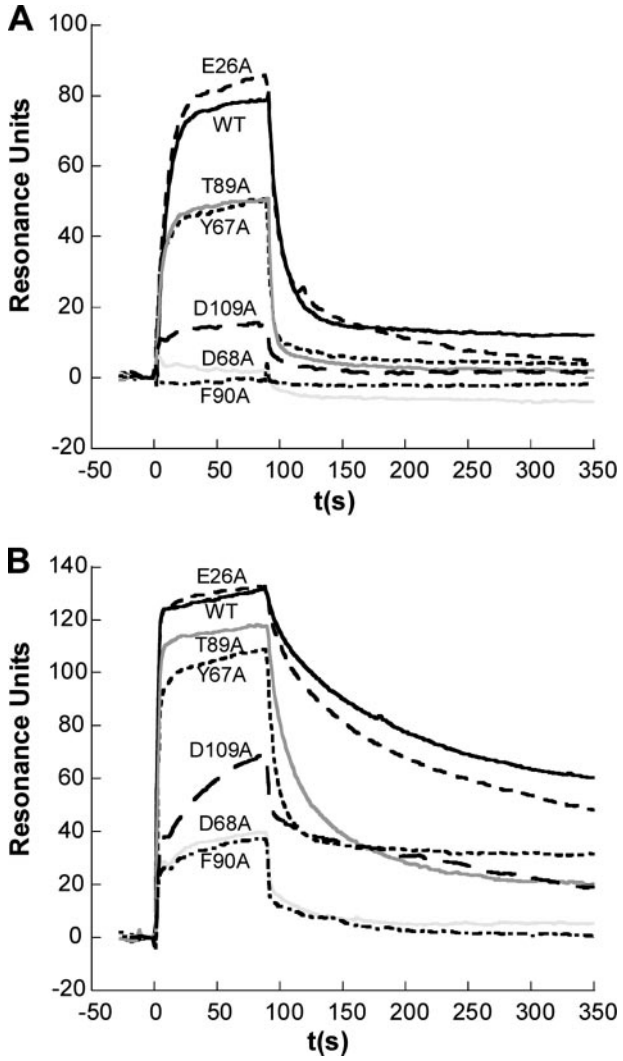

FIGURE 5. **BIAcore analysis of the binding of PCPE-1 and its mutant forms to immobilized mini-procollagen III in the absence (*A*) and presence (*B*) of 5 mM calcium.** Mini-procollagen III was covalently coupled to one flow cell of a CM4 sensor chip (305 resonance units). A control flow cell was similarly prepared but in the absence of added protein. His-tagged, recombinant human PCPE-1 in HBS-P (*A*) or HBS-*p* plus 5 mM $CaCl_2$ (*B*) buffer was injected simultaneously over both flow cells (flow rate 60 μl/min) and the response (resonance units) automatically calculated from the difference in signals. Dissociation was measured by injection of buffer alone. Wild-type PCPE-1 or its mutant forms were sequentially injected, at a fixed concentration of 100 nM, over the same mini-procollagen III surface, after regeneration with 2 M guanidinium chloride (*A*) or 0.25 M EDTA followed by 2 M guanidinium chloride (*B*).

stants. Analysis of the data using the BIAevaluation 4.1 software showed a significant improvement of the quality of the fit for PCPE-1 when the "heterogeneous ligand" model was used instead of the basic 1:1 binding model. The reasons for this ligand heterogeneity (mini-procollagen III in this case) are not completely clear, but plausible explanations are: 1) some critical lysine in the ligand may be involved in cross-link formation with the sensor chip surface leading to a decreased activity for a part of the mini-procollagen III population; 2) there are two populations in the initial mini-procollagen III preparation (due for example to incomplete loading with calcium); and 3) there are two independent binding sites on the ligand. To test the first hypothesis, we immobilized an anti-c-Myc antibody on the sensor chip, captured the mini-procollagen III which is c-Myc-tagged (28) and injected PCPE-1 as before. Capture was very stable (three c-Myc tags are present on one mini-procollagen III molecule), but even in this case, the "heterogeneous ligand" model was the most appropriate to fit the kinetic data. Consequently, the first hypothesis can be ruled out, but the last two hypotheses remain valid as the collagen triple helix has already been suspected to bind PCPEs (31) and mini-procollagen III could possibly offer several binding sites to PCPE-1.

TABLE 2
Dissociation constants of PCPE-1 and its mutants for mini-procollagen III

Constants were determined after analysis of the curves obtained by surface plasmon resonance with at least six different concentrations of PCPE-1 (and mutants) after immobilization of 305 resonance units of mini-procollagen III. The data were obtained in the absence of calcium and analyzed with BIAevaluation 4.1 software (BIAcore). Two models ("1:1 Binding with mass transfer" and "Two-state reaction") could be excluded based on preliminary controls performed according to the recommendations of the manufacturer. Other models were used to fit the data and the best fits were always obtained with the "Heterogeneous Ligand" model.

	PCPE-1	E26A	Y67A	D68A	T89A	F90A	D109A
K_{D1} (nM)	1.8	1.8	12	ND[a]	46	ND	66
K_{D2} (nM)	48	118	188	ND	274	ND	689
Chi2	0.814	2.19	4.84		4.19		1.66

[a] ND, not determined.

The dissociation constants obtained for the interaction between PCPE-1 and mini-procollagen III with the "heterogeneous ligand" model were 1.8 and 48 nM (Table 2). The first constant is in agreement with the value obtained for the interaction between procollagen I and PCPE-1 (1.1 nM (35)), although the kinetic parameters differ (k_{on} and k_{off} are, respectively, 16-fold and 26-fold higher). The same analysis was performed with the various mutants except for D68A and F90A, for which the kinetic constants were too high to be accurately fitted. Reliable fits were obtained for E26A (no change in K_{D1}; slight increase in K_{D2}) and D109A (36- and 15-fold increase in K_{D1} and K_{D2}, respectively, compared with wild type). For Y67A and T89A, statistical parameters were not as good as for the previous mutants but in agreement with previous results, deduced K_D values were significantly higher than for wild type and lower than for D109A. Determination of the dissociation constants in the presence of calcium gave less reliable data due to the strength of the interaction that hindered complete regeneration of the surface between injections.

Although calcium is clearly a key partner in the interaction between mini-procollagen III and PCPE-1, it is impossible to infer from previous data if calcium binds to mini-procollagen III, PCPE-1, or both. We have already shown that the C-propeptide of procollagen III binds calcium (35) and thus, mini-procollagen III like PCPE-1 is expected to bind calcium. To explore further the role played by calcium in PCPE-1, we monitored the effect of calcium binding on the intrinsic fluorescence of PCPE-1. As can be seen in Fig. 6*A*, the emission spectrum obtained with wild-type PCPE-1 has a maximum ~335 nm. Upon addition of a 40-fold excess of EGTA, the spectrum was not strongly modified, either because the protein does not contain calcium or because calcium cannot be removed by this treatment. Interestingly, however, when calcium is added to the EGTA-treated PCPE-1 (free concentration around 1.9 mM), the emission spectrum was blue-shifted and the peak area significantly decreased. The same type of behavior has already

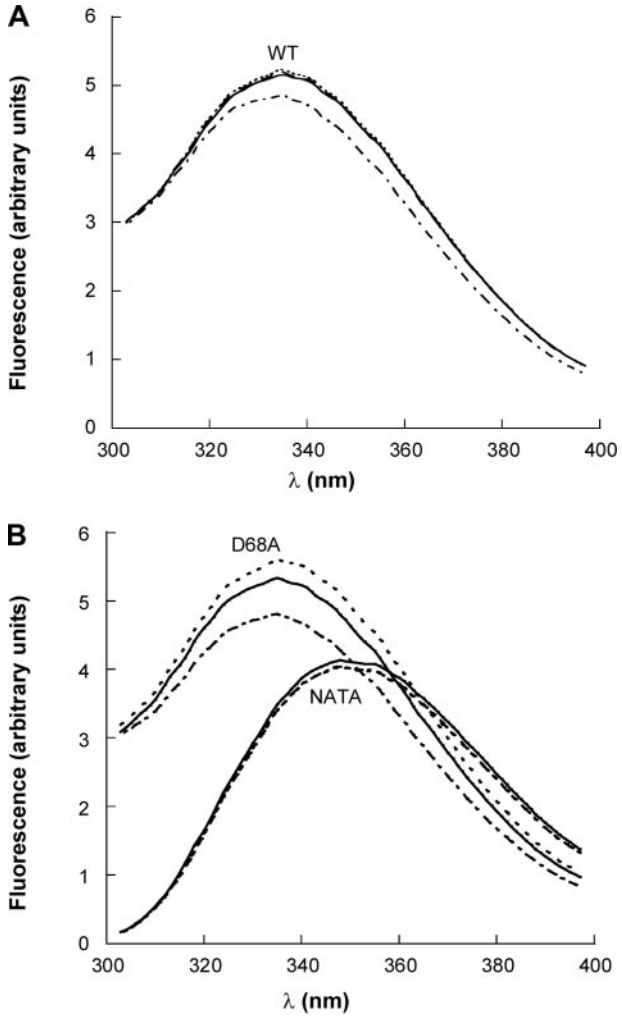

FIGURE 6. **Changes in intrinsic fluorescence observed upon calcium binding to PCPE-1 (*A*) and mutant D68A (*B*).** Solutions of protein (2.5 μM in 20 mM HEPES, pH 7.4, 0.15 M NaCl) were excited at 280 nm, and emission spectra were recorded between 295 and 400 nm (*continuous line*). EGTA (100 μM final concentration; *dotted line*) and $CaCl_2$ (1.9 mM final concentration; *dashed and dotted line*) were sequentially added, and spectra recorded 5 min after each addition. In the case of the wild-type (WT), the same experiment was also performed with $MgCl_2$ instead of $CaCl_2$ (*dashed line*; curve indistinguishable from EGTA treated). Total dilution in each case was less than 1%. In *B*, the spectra recorded with *N*-acetyl tryptophan amide (NATA) alone (*continuous line*), NATA plus 100 μM EGTA (*dotted line*) and NATA plus 100 μM EGTA plus 1.9 mM $CaCl_2$ (*dashed line*; curve indistinguishable from NATA plus EGTA) are also shown for comparison.

been observed for C1s, another CUB-containing protein for which calcium binding has clearly been demonstrated (20, 45). When the experiment was performed with $MgCl_2$ instead of $CaCl_2$, no change in fluorescence was observed (Fig. 6*A*) indicating that the changes observed with calcium were specific to this ion.

In contrast to wild-type PCPE-1, D68A seemed to be sensitive to both EGTA and Ca^{2+} (Fig. 6*B*), because EGTA caused an increase in intrinsic fluorescence, whereas $CaCl_2$ caused a large diminution of the peak area. This probably indicates that calcium is more labile in D68A compared with wild-type PCPE-1, but even the wild-type does not seem to be completely loaded with calcium in our conditions (no calcium present during the purification). Interestingly, other mutants supposedly involved in calcium binding or close to the calcium site (Y67A and D109A) displayed spectra similar to D68A, whereas mutants of the specific residues T89A and F90A behaved like wild type (data not shown).

DISCUSSION

We recently demonstrated that PCPEs are more specific than the tolloid proteases they activate (28), and because their action is solely on fibrillar procollagens, we proposed that PCPEs could be interesting targets to develop new anti-fibrotic therapies. This will require a better knowledge of the structural features that allow PCPEs to bind to procollagens, and the work described here is aimed at identifying residues in the CUB1 domain of PCPEs involved in the interaction with procollagens I–III.

Identification of regions involved in procollagen binding was hindered by the lack of high resolution structural data for PCPE-1. It is known that tolloid protease-enhancing activity is a property of the CUB domain-containing region (34, 46). Furthermore, data from our laboratory[4] have shown that proteolytic cleavage within the CUB1 domain leads to loss of PCPE function. In addition, others have shown the importance of surface-exposed loops connecting β-strands in the interactions of CUB domains in neuropilin-1 (7) and MAp19 (21). In the light of these observations, we decided to focus on residues in connecting loops that were either conserved in CUB domains or specific to the CUB1 domains in PCPEs.

Among the conserved residues, the most prominent effects were obtained when the acidic residues Asp-68 and Asp-109, two putative calcium ligands, were individually mutated to neutral alanines. Moreover, we demonstrate here that calcium affects the local structure of PCPE-1 and that this effect cannot be reproduced with another ion sharing similar properties such as magnesium. This supports the previous hypothesis (20) that PCPE CUB domains belong to the subset of CUB domains that bind calcium and that this ion is necessary to maintain their structural integrity. Although the putative calcium binding site is found in about two-thirds of the CUB domains, this ability to bind calcium was only discovered recently with the crystal structure of the CUB1-EGF fragment of C1s (20). Other such CUB domains are found in the complement proteases C1s, C1r and MASPs, the tolloid enzymes, the inflammatory GAG-binding protein tumor necrosis factor-stimulated gene *6* (TSG-6) and in receptors such as cubilin and neuropilins (Fig. 2).

Crystal structures have revealed that the exact nature of the calcium-binding residues and the involvement of side-chain and/or main-chain carbonyls are subject to variations from one CUB domain to another. For example, the aspartate homologous to PCPE Asp-68 contributes one (MAp19) or two (C1s) ligands, and the aspartate homologous to Asp-109 can be involved through its side chain (MAp19) or through its main chain (C1s). This raises the question of whether calcium ligands can also develop electrostatic contacts with the interacting partner of the CUB domain. This question was discussed by Gregory and colleagues (21) who concluded in favor of a disruption in structural integrity rather than of a key interaction of the CUB domain with the partner to explain the drops in affinity observed upon mutation of some calcium ligands. The iden-

[4] B. Font, C. Moali, D. Eichenberger, and D. J. S. Hulmes, unpublished observations.

tification of the exact nature and role of the calcium ligands in the CUB1 module of PCPEs will certainly require more investigation, because the full-length PCPEs are not the most appropriate tools to distinguish between the role of the calcium ion in CUB1 *versus* CUB2. Production of the CUB1 domain alone is in progress and should help to dissect the structure-function relationships in this particular domain. What is already clear, however, is the major role played by calcium ions in CUB domains. This is illustrated by the occurrence of several mutations in calcium ligands in CUB2, CUB3, and CUB4 of *Drosophila* tolloid, leading to disruptions in dorso-ventral patterning (47, 48), as well as in CUB1 of human MASP-2, resulting in chronic inflammatory disease (49). These mutations have been shown to impede tolloid function (43, 50) and formation of the MASP-2/mannan binding lectin complex (21, 49), respectively.

We also probed the role of tyrosine 67, a well conserved residue immediately preceding Asp-68. Mutation of the homologous residue in MAp19 was shown to yield the most pronounced effect on dissociation constants for MBL and L-ficolin among a series of 12 mutants (21) and to be directly involved in the interaction with the binding partners. In our case, the effect of replacing Tyr-67 by alanine was significant and reproducible but not as severe as in the case of MAp19. This result seems to indicate that, in some cases, conserved residues can influence differently the structure and activity of CUB domains even though they maintain a conserved framework of structural features. In the CUB1 domain of PCPE-1, the interaction mediated by Tyr-67 may not be as strong as in MAp19.

One of the most striking results in this study was the demonstration that phenylalanine 90 is a major determinant of PCPE-enhancing activity, and of the PCPE-1/procollagen III interaction, probably through hydrophobic contacts. We also note that mutation of threonine 89 led to a reduction in binding, and a small drop in enhancing activity. It is possible that this residue is involved in a hydrogen-bonding network that stabilizes the PCPE interaction site. We note that the sequence CGTFRP, including Thr-89 and Phe-90, is completely conserved in fish, frog, rodent, and human PCPEs (not shown), suggesting an important functional role. In contrast, PCPE-1 mutant E26A was found to stimulate BMP-1 activity at least as much as wild type. Because Glu-26 is diametrically opposite to Phe-90 in the three-dimensional structure, this may help to delineate the surface most probably involved in procollagen binding. We note that Glu-26 is adjacent in the three-dimensional structure to the N-terminal sequence of PCPE-1.

The agreement between the observed changes in PCPE-enhancing activity and binding to the mini-procollagen III substrate is striking. The mutants can be ranked in the same order in both assays. These data support the notion that the mechanism of action of PCPE involves binding to the BMP-1 substrate, although binding to the enzyme cannot be excluded (36).

Interestingly, mutations within adjacent loops in the neuropilin-1 CUB1 domain also resulted in dramatic decreases in the affinity of this receptor for class 3 semaphorins (7). These mutations are also located on the upper face of the CUB domain (see Fig. 1), in loops L3, L5, and L9, whereas a mutation in loop L2 on the lower face had no effect. Phenylalanine 90 in PCPE-1 CUB1 is also located on the upper face, but in loop L7. Similarly, residues involved in CUB domain interactions in *Drosophila* tolloid (50) and MAp19 (21) are located on the upper face, containing the calcium binding site. Based on these observations, we propose that the CUB L3, L5, L7, and L9 loops first defined in spermadhesins (41), and subsequently found in the calcium-binding CUB domains of C1s (20) and MAp19 (21), are the principal regions involved in ligand binding.

Although the loop regions in CUB domains seem to be required for ligand binding, the less mobile β-sheets appear to be involved in homo- (20, 21) and hetero-dimerization (41). In contrast to complement proteases and spermadhesins, however, PCPEs do not seem to form dimeric structures, as revealed by small angle x-ray scattering, even at the high concentrations required for data collection (51). The ability of CUB domains to form multimers may therefore be a versatile property of CUB-containing proteins that depends on the nature of the CUB module and on available partners for multimerization in a given physiological context. Thus, even though binding modes seem to be conserved among calcium-containing CUB domains, specific functions may result from different sets of residues in loops and β-strands and through a choice of functional modules located on either side of the CUB domain (EGF, CUB, NTR, and others).

We have previously shown that PCPE-1 binds to procollagen I with a K_d of 1.1 nM (35), but the one or more binding sites in procollagens are not known. Interestingly, PCPE-1 also binds both cleavage products released by BMP-1, pN-collagen, and the C-propeptide trimer. Because we have recently demonstrated that most of the triple helix can be removed without affecting PCPE activity (28), it is tempting to speculate that PCPEs bind to both the C-propeptide and the C-telopeptide, thereby inducing a conformational change in the procollagen molecule. The natural occurrence of shorter fragments of PCPE-1 that retain their enhancing activity despite the loss of the NTR domain allowed the demonstration that CUB domains alone are sufficient to enhance PCP activity (33, 34). Although the requirement for both CUB1 and CUB2 domains has never been challenged, this study showing that a single mutation in CUB1 can severely reduce the activity of PCPE-1, without affecting the overall structure of the protein, clearly demonstrates that CUB1 is required for enhancing activity. Even though the role of the CUB2 domain remains completely unexplored, we hypothesize that one PCPE CUB domain could bind to the C-propeptide and the other to the C-telopeptide in agreement with the size and shape of the various partners (51, 52). Future work will focus on which CUB domain binds to which side of the BMP-1 cleavage site and where in the C-telopeptide/C-propeptide the interaction sites are located. In the light of the results described here, especially the necessity for the specific residue Phe-90 in maintaining enhancing activity, it seems unlikely that CUB1 can be exchanged with another CUB domain, for example PCPE-1 CUB2, without loss of activity, but this remains to be demonstrated.

Acknowledgments—We are grateful to Alexandre Pozza and Attilio di Pietro for their help during the fluorescence experiments and to Gérard Arlaud and Nicole Thielens for helpful discussions.

REFERENCES

1. Gaboriaud, C., Thielens, N. M., Gregory, L. A., Rossi, V., Fontecilla-Camps, J. C., and Arlaud, G. J. (2004) *Trends Immunol.* **25,** 368–373
2. Sorensen, R., Thiel, S., and Jensenius, J. C. (2005) *Springer Semin. Immunopathol.* **27,** 299–319
3. Lee, H. X., Ambrosio, A. L., Reversade, B., and De Robertis, E. M. (2006) *Cell* **124,** 147–159
4. Davidson, G., Mao, B., del Barco Barrantes, I., and Niehrs, C. (2002) *Development* **129,** 5587–5596
5. Greenspan, D. S. (2005) *Top. Curr. Chem.* **247,** 149–183
6. Neufeld, G., Cohen, T., Shraga, N., Lange, T., Kessler, O., and Herzog, Y. (2002) *Trends Cardiovasc. Med.* **12,** 13–19
7. Gu, C., Limberg, B. J., Whitaker, G. B., Perman, B., Leahy, D. J., Rosenbaum, J. S., Ginty, D. D., and Kolodkin, A. L. (2002) *J. Biol. Chem.* **277,** 18069–18076
8. Reigstad, L. J., Varhaug, J. E., and Lillehaug, J. R. (2005) *FEBS J.* **272,** 5723–5741
9. Topfer-Petersen, E., Romero, A., Varela, P. F., Ekhlasi-Hundrieser, M., Dostalova, Z., Sanz, L., and Calvete, J. J. (1998) *Andrologia* **30,** 217–224
10. Tao, Z., Peng, Y., Nolasco, L., Cal, S., Lopez-Otin, C., Li, R., Moake, J. L., Lopez, J. A., and Dong, J. F. (2005) *Blood* **106,** 4139–4145
11. Milner, C. M., and Day, A. J. (2003) *J. Cell Sci.* **116,** 1863–1873
12. Zheng, Y., Mellem, J. E., Brockie, P. J., Madsen, D. M., and Maricq, A. V. (2004) *Nature* **427,** 451–457
13. Sugiyama, T., Kumagai, H., Morikawa, Y., Wada, Y., Sugiyama, A., Yasuda, K., Yokoi, N., Tamura, S., Kojima, T., Nosaka, T., Senba, E., Kimura, S., Kadowaki, T., Kodama, T., and Kitamura, T. (2000) *Biochemistry* **39,** 15817–15825
14. Christensen, E. I., and Gburek, J. (2004) *Pediatr. Nephrol.* **19,** 714–721
15. Hooi, C. F., Blancher, C., Qiu, W., Revet, I. M., Williams, L. H., Ciavarella, M. L., Anderson, R. L., Thompson, E. W., Connor, A., Phillips, W. A., and Campbell, I. G. (2006) *Oncogene* **25,** 3924–3933
16. Kang, W., and Reid, K. B. (2003) *FEBS Lett.* **540,** 21–25
17. Duke-Cohan, J. S., Tang, W., and Schlossman, S. F. (2000) *Adv. Exp. Med. Biol.* **477,** 173–185
18. Ge, W., Hu, H., Ding, K., Sun, L., and Zheng, S. (2006) *J. Biol. Chem.* **281,** 7406–7412
19. Wu, Q. (2003) *Curr. Top. Dev. Biol.* **54,** 167–206
20. Gregory, L. A., Thielens, N. M., Arlaud, G. J., Fontecilla-Camps, J. C., and Gaboriaud, C. (2003) *J. Biol. Chem.* **278,** 32157–32164
21. Gregory, L. A., Thielens, N. M., Matsushita, M., Sorensen, R., Arlaud, G. J., Fontecilla-Camps, J. C., and Gaboriaud, C. (2004) *J. Biol. Chem.* **279,** 29391–29397
22. Feinberg, H., Uitdehaag, J. C., Davies, J. M., Wallis, R., Drickamer, K., and Weis, W. I. (2003) *EMBO J.* **22,** 2348–2359
23. Bond, J. S., and Beynon, R. J. (1995) *Protein Sci.* **4,** 1247–1261
24. Ge, G., and Greenspan, D. S. (2006) *Birth Defects Res. C. Embryo. Today* **78,** 47–68
25. Ge, G., and Greenspan, D. S. (2006) *J. Cell Biol.* **175,** 111–120
26. Muraoka, O., Shimizu, T., Yabe, T., Nojima, H., Bae, Y. K., Hashimoto, H., and Hibi, M. (2006) *Nat. Cell Biol.* **8,** 329–338
27. Scott, I. C., Blitz, I. L., Pappano, W. N., Maas, S. A., Cho, K. W., and Greenspan, D. S. (2001) *Nature* **410,** 475–478
28. Moali, C., Font, B., Ruggiero, F., Eichenberger, D., Rousselle, P., Francois, V., Oldberg, A., Bruckner-Tuderman, L., and Hulmes, D. J. S. (2005) *J. Biol. Chem.* **280,** 24188–24194
29. Petropoulou, V., Garrigue-Antar, L., and Kadler, K. E. (2005) *J. Biol. Chem.* **280,** 22616–22623
30. Adar, R., Kessler, E., and Goldberg, B. (1986) *Collagen Rel. Res.* **6,** 267–277
31. Steiglitz, B. M., Keene, D. R., and Greenspan, D. S. (2002) *J. Biol. Chem.* **277,** 49820–49830
32. Steiglitz, B. M., Kreider, J. M., Frankenburg, E. P., Pappano, W. N., Hoffman, G. G., Meganck, J. A., Liang, X., Hook, M., Birk, D. E., Goldstein, S. A., and Greenspan, D. S. (2006) *Mol. Cell Biol.* **26,** 238–249
33. Kessler, E., and Adar, R. (1989) *Eur. J. Biochem.* **186,** 115–121
34. Hulmes, D. J. S., Mould, A. P., and Kessler, E. (1997) *Matrix Biol.* **16,** 41–45
35. Ricard-Blum, S., Bernocco, S., Font, B., Moali, C., Eichenberger, D., Farjanel, J., Burchardt, E. R., van der Rest, M., Kessler, E., and Hulmes, D. J. S. (2002) *J. Biol. Chem.* **277,** 33864–33869
36. Ge, G., Zhang, Y., Steiglitz, B. M., and Greenspan, D. S. (2006) *J. Biol. Chem.* **281,** 10786–10798
37. Combet, C., Jambon, M., Deleage, G., and Geourjon, C. (2002) *Bioinformatics* **18,** 213–214
38. Deleage, G., Combet, C., Blanchet, C., and Geourjon, C. (2001) *Comput. Biol. Med.* **31,** 259–267
39. Whitmore, L., and Wallace, B. A. (2004) *Nucleic Acids Res.* **32,** W668–W673
40. Divita, G., Di Pietro, A., Roux, B., and Gautheron, D. C. (1992) *Biochemistry* **31,** 5791–5798
41. Romero, A., Romao, M. J., Varela, P. F., Kolln, I., Dias, J. M., Carvalho, A. L., Sanz, L., Topfer-Petersen, E., and Calvete, J. J. (1997) *Nat. Struct. Biol.* **4,** 783–788
42. Kessler, E., and Goldberg, B. (1978) *Anal. Biochem.* **86,** 463–469
43. Hartigan, N., Garrigue-Antar, L., and Kadler, K. E. (2003) *J. Biol. Chem.* **278,** 18045–18049
44. Moschcovich, L., Bernocco, S., Font, B., Rivkin, H., Eichenberger, D., Chejanovsky, N., Hulmes, D. J. S., and Kessler, E. (2001) *Eur. J. Biochem.* **268,** 2991–2996
45. Thielens, N. M., Enrie, K., Lacroix, M., Jaquinod, M., Hernandez, J. F., Esser, A. F., and Arlaud, G. J. (1999) *J. Biol. Chem.* **274,** 9149–9159
46. Takahara, K., Kessler, E., Biniaminov, L., Brusel, M., Eddy, R. L., Janisait, S., Shows, T. B., and Greenspan, D. S. (1994) *J. Biol. Chem.* **269,** 26280–26285
47. Childs, S. R., and O'Connor, M. B. (1994) *Dev. Biol.* **162,** 209–220
48. Finelli, A. L., Bossie, C. A., Xie, T., and Padgett, R. W. (1994) *Development* **120,** 861–870
49. Stengaard-Pedersen, K., Thiel, S., Gadjeva, M., Moller-Kristensen, M., Sorensen, R., Jensen, L. T., Sjoholm, A. G., Fugger, L., and Jensenius, J. C. (2003) *N. Engl. J. Med.* **349,** 554–560
50. Canty, E. G., Garrigue-Antar, L., and Kadler, K. E. (2006) *J. Biol. Chem.* **281,** 13258–13267
51. Bernocco, S., Steiglitz, B. M., Svergun, D. I., Petoukhov, M. V., Ruggiero, F., Ricard-Blum, S., Ebel, C., Geourjon, C., Deleage, G., Font, B., Eichenberger, D., Greenspan, D. S., and Hulmes, D. J. S. (2003) *J. Biol. Chem.* **278,** 7199–7205
52. Bernocco, S., Finet, S., Ebel, C., Eichenberger, D., Mazzorana, M., Farjanel, J., and Hulmes, D. J. S. (2001) *J. Biol. Chem.* **276,** 48930–48936
53. Gouet, P., Courcelle, E., Stuart, D. I., and Metoz, F. (1999) *Bioinformatics* **15,** 305–308

Insights into How CUB Domains Can Exert Specific Functions while Sharing a Common Fold: CONSERVED AND SPECIFIC FEATURES OF THE CUB1 DOMAIN CONTRIBUTE TO THE MOLECULAR BASIS OF PROCOLLAGEN C-PROTEINASE ENHANCER-1 ACTIVITY

Guillaume Blanc, Bernard Font, Denise Eichenberger, Christophe Moreau, Sylvie Ricard-Blum, David J. S. Hulmes and Catherine Moali

J. Biol. Chem. 2007, 282:16924-16933.
doi: 10.1074/jbc.M701610200 originally published online April 19, 2007
